

On the polarimetry of coherent bremsstrahlung by photons' intensity spectra








S.Darbinyan,^a H.Hakobyan,^a R. Jones,^b A.Sirunyan,^a


H.Vartapetian^a

^a*2 Alikhanian Brothers str., EPD, Yerevan Physics Institute, 375036, Yerevan,
Armenia*




^b*University of Connecticut, Storrs, CT, USA*

Abstract

 The possibilities of the coherent bremsstrahlung (CB) polarimetry based on a shape analysis of the intensity spectra are discussed within the calculation methods presented. The influence of  different sources of uncertainty  including the choice of the atomic form-factors  (F) was analyzed. For  the working range of a CB spectrum an absolute accuracy of polarimetry  the level of 0.01-0.02 is re  able.

Key words: coherent,  bremsstrahlung, linear polarization, polarimetry

1 Introduction

As i  known the coherent bremsstrahlung of electrons in a crystal radiator is a basic method for  production of  intense, linearly polarized photon

* Corresponding author: Tel: +3741 355093, fax: +3741 398392 E-mail: Hrachya.Hakobyan@cern.ch

beams in the range of intermediate and high energies [1]. The present construction and development of a new powerful electron accelerators, running at high duty factors and intensities, creates a good opportunity for generation of highly polarized CB photon beams at the existing or especially constructed experimental facilities [2]. This allows to reach a high statistical accuracy of the data obtained, that in his turn assumes the need in a minimization of the systematic uncertainties coming in particular from the polarimetry sector.

Since CB experimental discovery in 60-ths, photon beams polarimetry has been mainly based on the known simple correlation between the CB intensity and polarization spectra [3] which allows to reduce the polarimetry to the measurement and shape analysis of the intensity spectra (so called CBSA-methods). A very few direct and precise measurements of the CB polarization were made exploiting both electromagnetic or nuclear processes. The earliest of them was carried out at DESY[4] for CB peak energy of 2.05 GeV by means of mutual asymmetry measurement of e^+e^- coherent pair production in a diamond crystal. The data obtained established a fairly good agreement between both methods of polarimetry, although no measure of quantitative agreement has been presented.

The data for a CB peak energy of 300 MeV were recently obtained using analyzing power of coherent π^0 production on a ^4He [5] are also in good agreement with CBSA calculations, without however conclusions on the precision of calculation method which seems is better than 0.02-0.03. The use of nuclear reactions for the CB polarimetry is mainly restricted by strong decrease of the cross-sections with photons' energies compared to electromagnetic processes.

The general restriction for the direct polarimetry methods follows both from the low luminosity and analyzing power as well as from the need in

the operation and maintenance of a dedicated setup. From the other hand the measurements of a CB intensity spectra are always mandatory for the monitoring purpose of the running experiments and allow to determine the CB polarization in on-line mode of the operation, without additional apparatus usage.

In this paper we briefly present and discuss the CB polarimetry within the CBSA methods both existing and developed at YERPHI as well as the need in a new direct CB polarimetry.

2 Methods of CB polarization calculations on the base of Intensity spectra

In an introduction to this part Fig.1 shows the CB spectra of intensity and polarization of a 4.5 GeV electrons shutting the diamond crystal near the [100] axe. The working region (WR) around $E_{\gamma}^{peak}=1.1$ GeV is dominated by contribution of the reciprocal lattice nodes $(0\bar{2}2)$, $(0\bar{4}4)$, $(0\bar{6}6)$, $(0\bar{8}8)$ with the polarization vector perpendicular to the plane $[\vec{p}_e \vec{b}_1]$ (app. $[\vec{b}_1 \vec{b}_2]$) while contribution of nodes (022) , (044) , (066) , (088) and others with a polarization value small in the WR is more pronounced at the end of a CB spectrum as is seen in Fig.1. Expressions for CB intensity and polarization are presented in the Appendix 1.

The CBSA methods primarily use a fitting of the measured CB spectrum to the convolution of the theoretical intensity $I^{th}(x, \theta, \alpha)$ with the smearing function $r(\theta, \alpha)$ according to equation:

$$I^{exp}(x) = \int I^{th}(x, \theta, \alpha) W(\theta, \alpha) d\theta d\alpha \quad (1)$$

where $x = E_{\gamma}/E_e$ is relative energy of the radiated photon and $W(\theta, \alpha)$

describes the influence of different experimental factors on the CB spectra shape, such as the angular divergence of the primary electrons, collimation of the secondary photons, multiple scattering and non-perfectness of the crystal, energy resolution of experimental setup etc.

The smearing function is parameterized in the analytical form and free parameters are defined by means of the folding procedure. Polarization of experimental spectra is determined according to the expression:

$$P^{\text{exp}}(x) = \int P^{\text{th}}(x, \theta, \alpha) I^{\text{th}}(x, \theta, \alpha) W(\theta, \alpha) d\theta d\alpha / I^{\text{exp}}(x) \quad (2)$$

or

$$P^{\text{exp}}(x) = \int 2(1-x)\psi_3^c(x, \theta, \alpha) W(\theta, \alpha) d\theta d\alpha / I^{\text{exp}}(x) \quad (3)$$

that follows from the definitions of the CB polarization both theoretical and experimental [6,7] (see details in Appendixes A1, A2).

The quality of the fit and therefore accuracy of the parameters is defined by correctness of the smearing model applied and the right case allows to reach the precision of 0.01-0.02 in a polarization values [8,9]. However the evaluated precision does not imply the influence of a systematical uncertainties either of the theoretical origin (f.e. the choice of the atomic form-factors (AFF's)) or the experimental one (unpredictable beam angular structure, uncontrolled crystal damage and others).

We have investigated the achievable polarimetry precision and corresponding impact of a relevant systematic uncertainties using methods presented below.

3 Method 1

describes the reconstruction of the smearing function by its Fourier decomposition amplitudes defined through the Fourier spectra of the theoretical and experimental intensities [8].

The ideology is based on the assumption that all experimental factors smearing out the theoretical spectra, can formally be presented in a form of the function which depends in the scale of the energy variable only. Thus, equation (1) can be rewritten as

$$I^{\text{exp}}(x_0) = \int I^{\text{th}}(x)_{\theta, \alpha} W(x - x_0) dx \quad (4)$$

where $I^{\text{th}}(x)_{\theta, \alpha} = I^{\text{th}}(x, \theta, \alpha)$ is defined as theoretical intensity spectrum for fixed values of crystal angles (θ, α) . Correctness of the ideology is based on a small differences between the CB spectra within the width of the smearing function and possibility to express an angular variables through energy of discontinuity [6]. In analogy with equation (2) one can rewrite:

$$P^{\text{exp}}(x_0) = \int P^{\text{th}}(x)_{\theta, \alpha} I^{\text{th}}(x)_{\theta, \alpha} W(x - x_0) dx / I^{\text{exp}}(x_0) \quad (5)$$

The expression (4) is classified as a Fredholm's integral equation of the first type with the kernel $W(x - x_0)$ depending on a difference of the arguments only and may be solved by means of the integral Fourier transformation [10]. Making a Fourier transformation of both sides of eq.(4) is easy to find out the Fourier spectrum of the smearing function:

$$W(k) = (I^{\text{exp}}(k) / I^{\text{th}}(k)) / \sqrt{2\pi} \quad (6)$$

where $I^{\text{exp}}(k)$, $I^{\text{th}}(k)$ are the Fourier spectra of $I^{\text{exp}}(x)$ and $I^{\text{th}}(x)$ respectively. Using inverse Fourier transformation one can reconstruct $W(x)$.

Substituting the expression for $W(x)$ into (4) we may obtain the following expression for the polarization spectrum:

$$P^{exp}(x) = F^{-1}[PI(k)I^{ex}]/I^{exp}(x) \quad (7)$$

where $PI(k)$ is the Fourier spectrum of the product $P^{th}(x)I^{th}(x)$.

As is seen final expression (7) uses the Fourier decomposition amplitudes of the experimental and theoretical spectra only. There is no need for other information that is the main advantage of this approach.

4 Method 2 (simplified)

Based on two corrections introduced in the theoretical expression for $P^{th}(x, \theta, \alpha)$ (see A1.9). The first correction consists in the replacement of the coherent to incoherent ratio $I^{coh}(x, \theta, \alpha)/I^{inc}(x)$ by its experimental value $\beta^{exp} = I^{coh.exp}(x)/I^{inc.exp}(x)$ [11] to account for the relative changes in the coherent to incoherent ratio in the experimental spectrum due to the influence of the smearing factors (see Fig. 1):

$$P(x, \theta, \alpha) = \frac{2(1-x)\psi_3^c(x, \theta, \alpha)}{I^{th}(x, \theta, \alpha)} \frac{\beta^{exp}}{\beta^{exp} + 1} \quad (8)$$

where $I^{coh.exp}(x)$ and $I^{inc}(x)$ are the normalized coherent intensities of the experimental and theoretical spectra. The second one comes from the need to account for the relative change in the $(0\bar{2}2)$ contribution to the coherent intensity due to the relatively strong smearing of its shape as compared to weakly distorted tails of 044 , $0\bar{6}6$, $0\bar{8}8$ and other reflections from the high energy end. The correction factor is defined as a:

$$C(x) = 1 + (I^{coh.exp}(x) - I^{coh}(x))/I_1^{coh}(x) \quad (9)$$

where I_1^{coh} is the calculated $0\bar{2}2$ node's contribution and introduced into the expressions for the structure functions (see A1.5,6,8).

The polarization in V is dominated by decreasing contribution of nodes $0\bar{2}2$, $0\bar{4}4$, $0\bar{6}6$, $0\bar{8}8$, while the tails of the nodes exited at the end of CB spectra give practically unpolarized contribution I_{VR} and may be neglected in ψ_3^c (A1.8). With these modifications an expression (8) may be used for polarization calculation.

5 Scheme of calculations

First of all the methods presented were examined using a variety of Monte-Carlo(MC) simulated CB spectra for different peak energies ($x_{(0\bar{2}2)} = 0.2 - 0.5$), primarily for the conditions of γ -2 beam line of YERPHI's electron synchrotron ($E_e = 4.5$ GeV, diamond crystal thickness $80\mu\text{m}$, beam effective divergence app. 0.1 mrad, collimation 0.15 mrad (half aperture). In addition more distorted CB spectra were generated (collimation 0.3 mrad, average beam divergence 0.3-0.5 mrad) aimed to provide more crucial tests of the calculation methods presented.

As a first step in the polarization calculation the coherent theoretical spectrum was to be constructed for a given experimental spectrum according to the expression for $I^{th}(x, \theta, \alpha)$ (see (A1.5)). The choice of a crystal azimuthal angle θ is fixed to 0.05 mrad is defined by the energy of $0\bar{2}2$ discontinuity in theoretical spectrum, that may be approximated by the centre of linear decrease in the right side of the experimental one (Fig.1b) it is worth to mention the need in the careful construction of the theoretical spectrum in the case of the strong photon beam collimation ($\theta_k < m/E_e$) that should be realized within a known selection criteria of the contributing nodes in the reciprocal

lattice space for the point-like crystal target [1].

The second important step consists the evaluation and subtraction of CB incoherent contamination. The need in this operation corresponds to a possible in-consistence of incoherent background between theoretical and experimental spectra due either to a crystal radiation damage or electron beam touching the crystal's holder or radiation background of accelerator. The subtraction procedure is based on assumption that the ratio of the integrated coherent intensity for a wide regions of experimental spectrum $I^{exp}(x)$ is not disturbed by smearing factors and kept equal to the same in theoretical one. Using this assumption is possible to subtract and control the value of the incoherent contamination. The choice of the extended CB regions around WR ($x_{min} < x < x_{088}$) and in the plato ($0.65 < x < 0.8$) is convenient for this purpose (see Fig.1b). The relative weight of the coherent contamination in plato region does not ordinary exceed 10-20% which allows a good sensitivity of the mentioned ratio to the level of incoherent intensity subtracted. The region of 22, 044, 066 nodes with a visible shape's distortion is appropriate in the subtraction of the smearing function while the flat ones are weakly distorted and not informative for this purpose.

The equation (4) for the case of the incoherent component subtracted is replaced by:

$$I^{coh.exp}(x_0) = \int I^{coh}(x)_{\theta,\alpha} W(x - x_0) dx \quad (10)$$

where $I^{coh.exp}$ and I^{coh} are the coherent intensities of experimental and theoretical spectra. It is assumed that $W_c(x - x_0) = W(x - x_0)$ of equation (4).

The integral Fourier transformation was realized by means of the Fast Fourier Transformation (FFT) algorithm [12] requiring $N = 2^n$ points in the function discrete presentation. The choice of $N=64$ for our case allowed to cover

the region of the $0\bar{2}2$ and $0\bar{4}4$ reflections. Before the start of a Fourier analyses, the careful statistical smoothing of the regions of interest was realized, aimed to prevent an excess of a high frequency components in the decomposition spectra. Calculations have been done for seven types of atomic form-factors following to see the influence of the choice.

6 Results and discussion

The MC simulated CB spectra for $I^{exp}(x)$ and $P^{exp}(x)$ and corresponding data of the polarization obtained within method 1 and 2 are shown in Figs. 2-4 for a different peak energies. There is seen a good agreement between the MC and method 1 results within accuracy $\Delta P = 0.01$ in the range of $\Delta x/x \leq 0.6$, reaching 0.02 at the flat ends which are weakly distorted by smearing factors and have a low weight in the units of Figure of Merit (P^2).

Data within the method 2 agree as a whole satisfactorily with MC results. As is seen, an agreement is good at the peak energies above $x_{(0\bar{2}2)} \geq 0.3$ and even better than within method 1 at the flat end of the WR. The deterioration is observed toward to the lower x corresponding to a smaller α setting when an angular uncertainty $\Delta\alpha/\alpha$, responsible for the smearing size, reaches 0.35-0.4 at $x_{(0\bar{2}2)} = 0.22$ and collimation 0.3 mrad (see Fig. 2). However an observed deviation from the MC data does not exceed 0.02-0.03 in the range of $\Delta x/x \leq 0.2$. In the case of the smaller collimation, method 2 allows to obtain an accuracy of 0.01-0.02 in the wide WR ($\Delta x/x \leq 0.6$) of peak energies $0.2 \leq x_{(0\bar{2}2)} \leq 0.5$.

We have investigated different sources of systematic uncertainties having impact on the polarization calculation:

Choice of Atomic Form-factor.

Atomic form-factors (AFF) enter the CB polarimetry models which exhibit an atomic nuclei as a target. The data obtained so far in ref. [4,13] for the diamond and silicon crystals confirm the preference of the Hartree-Fock (HF) type form-factors in the descriptions of a CB spectra. However the definite conclusion and finalization of the AFF type is expected in particular for the light nuclei. We have investigated the relative influence of different AFF's choice to a polarization calculation. Fig. 5a shows the part of the CB density spectrum $x_{(0\bar{2}2)} = 0.22$ measured by a 3-channels pair spectrometer [14] and corresponding polarization spectra (Fig. 5c) obtained for a few selected AFF models: namely exponential, Molier, HF, Dirac-Slater wave functions based HF, relativistic HF and the latest shell model based HF respectively (see ref.[14,15]).

As an important result there is seen a coincidence of all polarization spectra in the WR of $\Delta x/x \leq 0.6$ within accuracy ≤ 0.05 that is also clearly confirmed in the plot of the differences $(P_i(x) - P_{D-T}(x))$ (Fig. 5d), where $P_{D-T}(x)$ is contributed to the use of the Doyle-Turner AFF [15e]. The sensitivity in the choice of AFF becomes more noticeable in the right side of WR that may be interpreted as a dominance of $(0\bar{2}2)$ node in the CB peak region and a different dependence of AFF's on the momentum transfer to the crystal lattice, more pronounced in the right side of a WR, in particular in the zone of $(0\bar{4}4)$ node excitation.

As is seen from Fig. 5c the data obtained with AFF's mentioned are divided into two groups by their closest. The first group involves an Exponential and Moliere AFF's while the second one contains others. The similar results were also obtained for the WR around $x_{(0\bar{2}2)} = 0.5$.

Uncertainty in the definition of the peak energy.

The variation of a $x_{0\bar{2}2}$ position within 5-10% for the theoretical spectrum

Construction is immediately responding in the position shift of the smearing function. However it has no visible influence within accuracy of $\Delta P \leq 0.005$ on the calculated polarization values. The plot of the smearing function $W(x)$ fitted by Gaussian, is shown in Fig. 5 extracted from experimental spectrum plotted in Fig. 5a. As is seen from figure, $W(x)$ is positioned satisfactorily symmetric to the zero, indicating the correctness of $x_{(0\bar{2}2)}$ choice.

Choice of a different widths of the CB regions.

Two new selections were considered and used as for the incoherent contamination subtraction as well as for FFT algorithm application ($N = 64-128$). The results obtained didn't show a visible influence within accuracy of $\Delta P \leq 0.005$ on the polarization values.

Smoothing influence.

It was investigated for the case of a statistical fluctuations level in the level of $\leq 5\%$ in the intensity spectra. The results obtained show that smoothing doesn't affect the shape of CB peak, its maximum with a corresponding increase in the calculated polarization to $\Delta P \leq 0.005$, so it was applied for the relatively flat zones only.

7 Conclusion

As one may conclude, the CBSA methods are able to provide the polarimetry precision at the level of $\Delta P \leq 0.02$ within the investigated CB peak energy range $\omega_{22} = 0.2-0.5$. The extension of a CBSA validity zone with this accuracy and its absolute calibration require a correct choice of AFF type that is possible to realize by a simultaneous application of the direct polarimetry method with the expected precision $\Delta P \leq 0.02$ in parallel with the measurement of a CB spectra [16].

The polarization data obtained should be coincident for both polarimetry methods if the AFF's choice is correctly done. With this verification the CBSA methods, we believe meet the requirements of the modern experimental studies.

This work has been supported by CRDF grant AP2-2305-YE-02.

References


- [1] M.L.Ter-Mikaelian, Zh. Eksp. Teor. Fiz. **25**(1953)296
H.Uberall, Phys.Rev. **103**(1956)1055
G.Bologna et al., IL Nuov.Cim. **A**, **XLII**, N4(1966)844
- [2] see for example Proceedings of NSTAR-2001 (Workshop on the physics of excited nucleons, Mainz, 7-10 March 2001) and references therein.
- [3] G.Diambrini-Palazzi, Rev. Mod. Phys **40**,N3(1968)611
- [4] L.Criegee et al., Phys. Rev. Lett. **16**(1966)1031
- [5] A.Kraus et al., Phys. Rev. Lett. **79**(1997)3834
- [6] U.Timm, Fortschr. Phys. **17**(1969)765
- [7] J.Ahrens, Proceedings of Workshop "Polarized Photon Polarimetry", 2-8 June1998, Newport News, Virginia, CLAS-Note(CEBAF), 98-018, p.8
- [8] H.Hakobyan et al., Preprint YERPHI-908(59)-86,1986
- [9] L.Ya.Kolesnikov et al., Ukrainian Phys. J. **29**(1984)1296
- [10] A.G.Sveshnikov and A.I.Tikhonov, Theory of functions of complex variables, Published by "Nauka",Moscow,1974
- [11] H.Hakobyan and G.Karapetyan, Preprint YERPHI-1138(15)-89,1989
- [12] L.Rabiner and B.Gold, Theory and application of signals' digital processing, Published by "Mir", Moscow, 1978
- [13] I.Endo et al., Phys. Rev. Lett.**60**(1988)2292
- [14] F.Adamyan et al., Eur. Phys. J. **A8**(2000)423
- [15] a. Y.S.Tsai, Rev.Mod.Phys **46**, N4(1974)815

b. E.A.Dahl, Preprint Bonn-IR-82-26,1982



c. D.T.Cromer and J.T.Waber, Acta. Crystallogr. **A18**(1968)104

d. D.T.Cromer and J.B.Mann, Acta.Crystallogr. **A24** (1968)321






e. P.A.Doyle and P.S.Turner, Acta.Crystallogr. **A24**(1968)390

g. F.P.Korshunov and A.P.Lazar, Yad. Fiz. **66**(2003)442  F.Adamyan et al.,
Preprint YERPHI-1590(11)-03,2003(to be submitted to NIM)

Appendix 1

The  weighted Intensity $I^{th}(x, \theta, \alpha)$ is related to the bremsstrahlung cross-section $d\sigma(x, \theta, \alpha)/dx$ as 



$$I^{th}(x, \theta, \alpha) = \int d\sigma(x, \theta, \alpha)/dx \quad (\text{A1. 1})$$

where $x = E_\gamma/E_e$ is the ratio of radiated photon energy  the electron one, θ and α are the azimuthal and polar angles defined relative to crystallographic axes as  is shown in Fig. 1a.  Intensity I^{th} is defined as a sum of coherent ( I^{coh}) and incoherent ( I^{inc}) components of CB spectrum:

$$I^{th}(x, \theta, \alpha) = I^{coh}(x, \theta, \alpha) + I^{inc}(x) \quad (\text{A1. 2})$$

$$I^{coh}(x, \theta, \alpha) = [1 + (1 - x)^2] \psi_1^c(x, \theta, \alpha) - (2/3) (1 - x) \psi_2^c(x, \theta, \alpha) \quad (\text{A1. 3})$$

$$I^{inc}(x) = [1 + (1 - x)^2] \psi_1^{am} - (2/3) (1 - x) \psi_2^{am} \quad (\text{A1. 4})$$

where structure functions $\psi_1^c(x, \theta, \alpha)$  $\psi_2^c(x, \theta, \alpha)$ are defined as 

$$\psi_1^c(x, \theta, \alpha) = \frac{(2\pi)^2}{2a^3} \delta \sum_g |S(g)|^2 e^{-Ag^2} F(g^2) \frac{g_2^2 + g_3^2}{g_{||}^2} \quad (\text{A1. 5})$$



$$\psi_2^c(x, \theta, \alpha) = 3 \frac{(2\pi)^2}{a^3} \delta^2 \sum_g |S(g)|^2 e^{-Ag^2} F(g^2) \frac{(g_2^2 + g_3^2)(g_{||} - \delta)}{g_{||}^4} \quad (\text{A1. 6})$$

$\psi_1^{nc}(x) \sim 18.2$, $\psi_2^{inc}(x) \sim 17.4$ for the case of the full form [1].

where:

$a = 922$ is the constant of the diamond crystal lattice (in units of electron's Compton wavelength), $\vec{g}(g_1, g_2, g_3)$ - vector of reciprocal lattice,

$g_{\parallel} = g_2 \cos \alpha + g_3 \sin \alpha$ - projection of reciprocal lattice vector on the direction of electron,

$\delta = \frac{c^2}{E_e} \frac{x}{1-x}$ - minimum momentum transfer nuclei (lattice), $S(g)$ - structure factor - Debye-Waller factor, $F(g^2)$ - atomic form-factor.

The value for the linear polarization is expressed through a ratio of ψ_3^c structure function to the full intensity as

$$P^{th}(x, \theta, \alpha) = \frac{2(1-x)\psi_3^c(x, \theta, \alpha)}{I^{th}(x, \theta, \alpha)} \quad (\text{A1. 7})$$

where structure function ψ_3^c is written as a:

$$\psi_3^c(x, \theta, \alpha) = -\frac{(2\pi)^2}{a^3} \delta^3 \sum_g |S(g)|^2 e^{-Ag^2} F \frac{[(g_2^2 - g_3^2) \cos 2\alpha + 2g_2g_3 \sin 2\alpha]}{g_{\parallel}^4} \quad (\text{A1. 8})$$

(A1.8) For definition of polarization see Appendix 2.

For the polarization calculation we also use a transformed expression

(A1.7):

$$P^{th}(x, \theta, \alpha) = \frac{2(1-x)\psi_3^c(x, \theta, \alpha)}{I^{coh}(x, \theta, \alpha)} \frac{\beta}{\beta + 1} \quad (\text{A1. 9})$$

where $\beta = I^{coh}/I^{inc}$ is the ratio of the coherent to incoherent CB contribution

Appendix 2

theoretical expression for CB polarization is defined as a:

$$P^{th}(x, \theta, \alpha) = \frac{I_{\perp}^{th} - I_{\parallel}^{th}}{I^{th}} = \frac{I_{\perp}^{coh} - I_{\parallel}^{coh}}{I^{th}} \quad (\text{A2. 1})$$

where I_{\perp}^{th} and I_{\parallel}^{th} are the components of the photons radiation intensity $I^{th} = I_{\perp}^{th} + I_{\parallel}^{th}$ with polarization vector perpendicular (parallel) to the $plane \vec{b}_1$] (see Fig. 1) and each intensity component may be conventionally decomposed into the coherent and incoherent parts:

$$I_{\perp, \parallel}^{th} = I_{\perp, \parallel}^{cth} + \frac{1}{2} I_{\perp, \parallel}^{cth} \quad (\text{A2. 2})$$

In analogy with the expression (A2.1) one may define an experimental polarization as

$$P^{exp}(x) = \frac{I_{\perp}^{exp} - I_{\parallel}^{exp}}{I^{exp}} \quad (\text{A2. 3})$$

where $I_{\perp}^{exp}, I_{\parallel}^{exp}$ are the components of the experimental intensity $I^{exp} = I_{\perp}^{exp} + I_{\parallel}^{exp}$, which could be expressed through the theoretical ones according to a general equation (1) (see in the text):

$$I_{\perp, \parallel}^{exp}(x) = \int I_{\perp, \parallel}^{th}(x, \theta, \alpha) W(\theta, \alpha) d\theta d\alpha \quad (\text{A2. 4})$$

With this definition and without use of the "factorization" hypothesis [6.7] one may rewrite expression (A2.3) as

$$P^{exp}(x) = \frac{\int (I_{\perp}^{th} - I_{\parallel}^{th}) W(\theta, \alpha) d\theta d\alpha}{I^{exp}(x)} \quad (\text{A2. 5})$$

and taking into account the definition (A2.1) obtain a final expression:

$$P^{exp}(x) = \frac{\int (P^{th}(x, \theta, \alpha) I^{th}(x, \theta, \alpha) W(\theta, \alpha) d\theta d\alpha)}{I^{exp}(x)} \quad (\text{A2. 6})$$